Impact of valence fluctuations on the electronic properties of RO_{1−x}F_{x}BiS_{2} (R=Ce and Pr)

S. Dash, T. Morita, K. Kurokawa, Y. Matsuzawa, N. L. Saini, N. Yamamoto, Joe Kajitani, R. Higashinaka, T. D. Matsuda, Y. Aoki, and T. Mizokawa

Impact of valence fluctuation on electronic properties of REO$_{1-x}$F$_x$BiS$_2$ (RE = Ce and Pr)

S. Dash,[1] T. Morita,[1] K. Kurokawa,[1] Y. Matsuzawa,[1] N. L. Saini,[2] N. Yamamoto,[3]
Joe Kajitani,[3] R. Higashinaka,[3] T. D. Matsuda,[3] Y. Aoki,[3] and T. Mizokawa[1]

[1]*Department of Applied Physics, Waseda University, Tokyo 169-8555, Japan*
[2]*Dipartimento di Fisica, Universitá di Roma "La Sapienza" - Piazzale Aldo Moro 2, 00185 Roma, Italy*
[3]*Department of Physics, Tokyo Metropolitan University, Hachioji 192-0397, Japan*
(Dated: September 10, 2018)

We have investigated the electronic properties of BiS$_2$-based superconductors using x-ray photoemission spectroscopy (XPS). In going from $x = 0.3$ to 0.5 in PrO$_{1-x}$F$_x$BiS$_2$, the Pr $3d$ and Pr $4d$ peaks are shifted by $\sim 0.10 \pm 0.05$ eV away from the Fermi level, partially consistent with the electron doping. In PrO$_{1-x}$F$_x$BiS$_2$, the Pr^{3+}/Pr^{4+} mixed valence remains unchanged with the electron doping from $x = 0.3$ to 0.5. In CeO$_{1-x}$F$_x$BiS$_2$, the doped electrons for $x = 0.5$ almost suppresses Ce^{3+}/Ce^{4+} valence fluctuation. Although the core level peaks are also shifted by $\sim 0.10 \pm 0.05$ eV towards higher binding energy side with the electron doping from $x = 0$ to 0.5 in CeO$_{1-x}$F$_x$BiS$_2$, the Bi $4f_{7/2}$ binding energy shift is higher in the Pr system compared to the Ce system. The present results suggest that the doped electrons increase orbital occupations in the rare earth $4f$ orbitals at the valence band and show valence fluctuation differently in the two systems.

I. INTRODUCTION

After the discovery of BiS$_2$-based superconductor in Bi$_4$O$_4$S$_3$ by Mizuguchi *et al.*[1] in 2012, extensive studies[2–4] including RE(O,F)BiS$_2$ systems (RE=rare earth element)[5–19] have been attained. RE(O,F)BiS$_2$ contains alternatively stacked REO$_{1-x}$F$_x$ block layer and BiS$_2$ layer, and conductivity is enhanced by increasing x in the block layer which introduces electrons to the electronically active BiS$_2$ layer to exhibit the superconductivity at low temperature.[21] The electric properties of RE(O,F)BiS$_2$ are governed by the Fermi surfaces constructed from the Bi $6p_x$ and $6p_y$ orbitals, whereas the magnetic properties are related to the RE $4f$ orbital occupation.[22–24] In addition, the strong electron-phonon coupling has been reported in Bi$_4$O$_4$S$_3$[3] and LaO$_{0.5}$F$_{0.5}$BiS$_2$.[25–28] On the other hand, spin and orbital fluctuation due to electron-electron interaction are seen with the Fermi surface nesting in LaO$_{0.5}$F$_{0.5}$BiS$_2$.[22] As quasi-one-dimensional Bi $6p_x/p_y$ character is involved with the Fermi surface nesting,[22,29] it would be quite interesting to investigate and understand the role of doped electrons in REO$_{1-x}$F$_x$BiS$_2$ superconductors.[30]

In CeO$_{1-x}$F$_x$BiS$_2$, for $x \leq 0.4$, the system is in the Ce^{3+}/Ce^{4+} valence fluctuation regime, while for $x > 0.4$ the system is in the Kondo regime where valence fluctuation is suppressed such that superconductivity and the long range ferromagnetic orderings (Ce-S-Ce super exchange) are appeared at low temperature.[31] This shows that the electron doping is crucial in controlling the superconductivity and the magnetism in BiS$_2$-based superconductors.[32] Angle resolved photoemission spectroscopy (ARPES) shows that the area of the Fermi surfaces in CeO$_{1-x}$F$_x$BiS$_2$ is inconsistent with the nominal

F.[33–35] This discrepancy between the doping level and the Fermi surface area suggests that some electrons are localized instead of contributing to the Fermi surfaces. Recently, a resonant ARPES study by Sugimoto *et al.* has shown that the added electrons to the Fermi surface rather increase the occupations to the localized Ce $4f$ orbital hybridized with the Bi $6p_z$.[36] This genuinely requires further support from the core level spectroscopy to elucidate the orbital occupations and valence state involved with the electron doping in CeO$_{1-x}$F$_x$BiS$_2$.

Compared to CeO$_{1-x}$F$_x$BiS$_2$, the electronic properties of PrO$_{1-x}$F$_x$BiS$_2$ are less studied. The system is semiconducting for $x = 0$, and superconductivity appears for $x = 0.1$ till 0.7 at low temperature.[16] T$_c$ is increased from 2.4 to 4.1 K by the electron doping from $x = 0.3$ to 0.5 in PrO$_{1-x}$F$_x$BiS$_2$.[18] The lattice parameter along c-axis is decreased by the electron doping as above. Although the presence of Pr^{3+}/Pr^{4+} valence fluctuation was reported in PrO$_{1-x}$F$_x$BiS$_2$ ($x = 0.13$, 0.23) using x-ray photoemission spectroscopy (XPS) by Ishii *et al*,[20] the XPS results were not analyzed quantitatively and the doping effects on the valence fluctuation were not clarified. In this paper, we have studied the core level photoemission spectra to elucidate the F doping effect and the Ce or Pr valence fluctuation in CeO$_{1-x}$F$_x$BiS$_2$ ($x = 0$, 0.5) and PrO$_{1-x}$F$_x$BiS$_2$ ($x = 0.3$, 0.5) in a quantitative way.

II. METHOD

High-quality single crystals of PrO$_{1-x}$F$_x$BiS$_2$ (x=0.3, 0.5) and CeO$_{1-x}$F$_x$BiS$_2$ ($x = 0$, 0.5) were prepared by CsCl flux method as described elsewhere.[17–19] The F doping level is given by nominal value.[17] Photoemission spec-
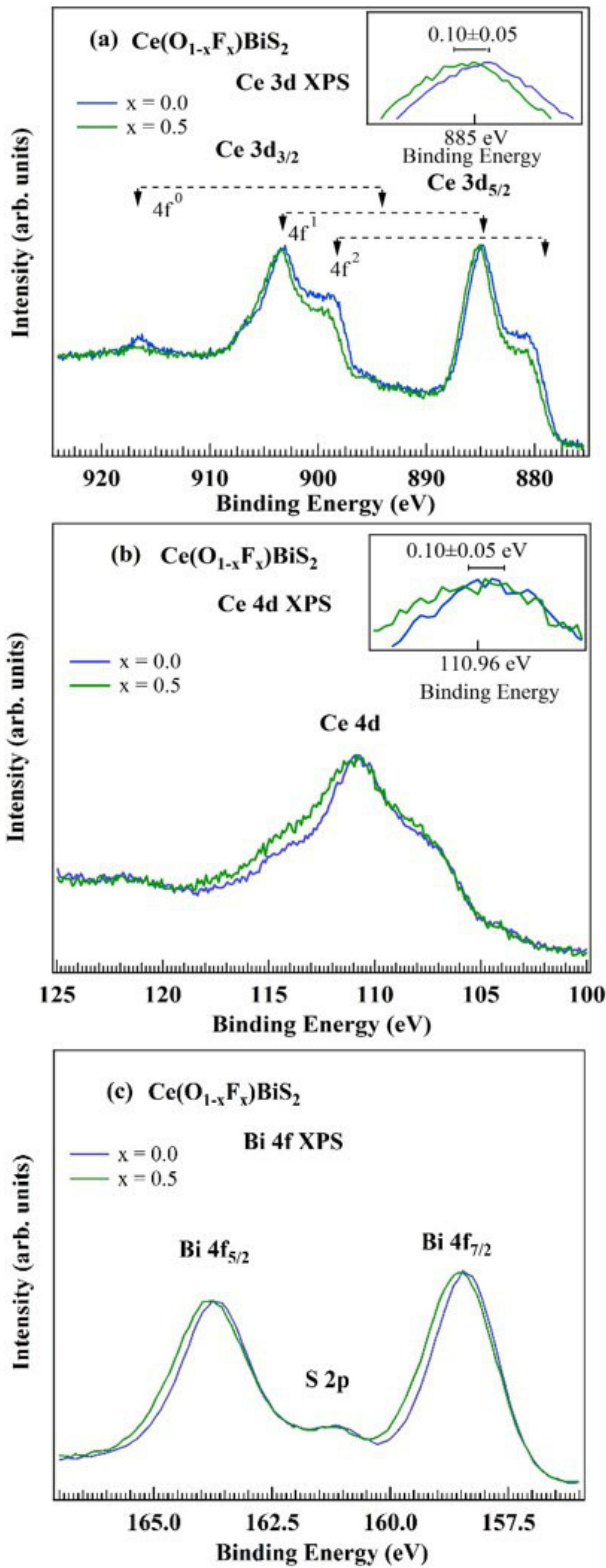
FIG. 1: (Color online) XPS of (a) Ce 3d, (b) Ce 4d, and (c) Bi 4f from $CeO_{1-x}F_xBiS_2$ ($x = 0, 0.5$) at room temperature.
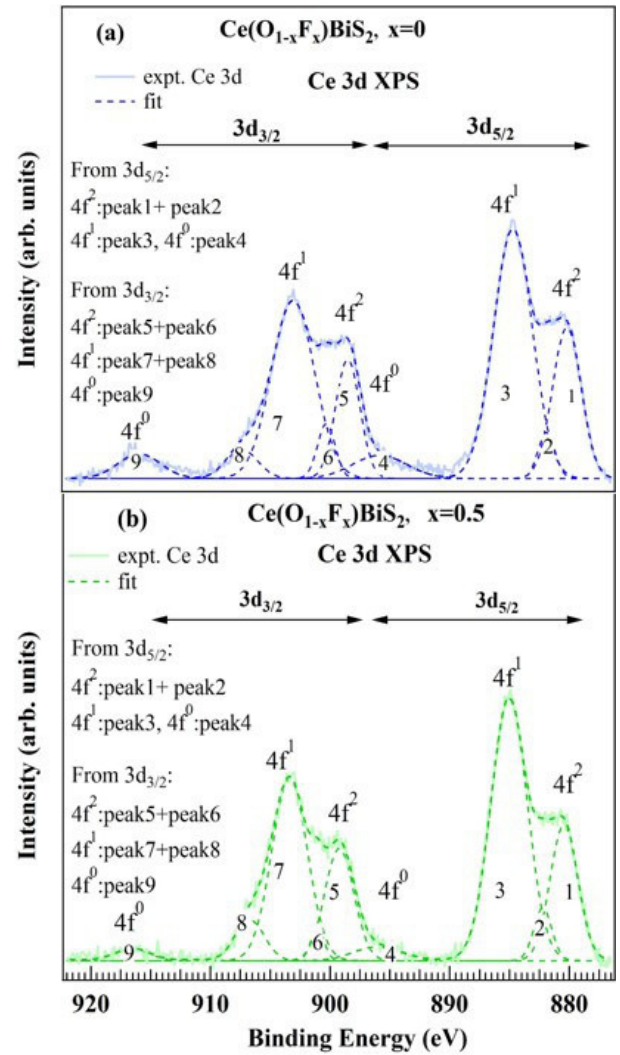
FIG. 2: (Color online) XPS of Ce 3d with Gaussian fittings from $CeO_{1-x}F_xBiS_2$ for (a) $x = 0$ and (b) $x = 0.5$ at room temperature.

troscopy at room temperature was carried out with JEOL JPS9200 analyzer using Mg Kα (1253.6 eV) source. The total energy resolution was about 1.0 eV. The base pressure of the measuring chamber was 2×10^{-6} Pa. Each spectrum is normalized with its peak intensity and binding energy is calibrated with Au 4f at 84.0 eV.

III.   RESULTS AND DISCUSSION

In Fig. 1(a), the Ce 3d peaks of $CeO_{1-x}F_xBiS_2$ ($x = 0, 0.5$) show shifting of $\sim 0.10 \pm 0.05$ eV towards higher binding energy from $x = 0$ to 0.5 as shown in the inset. The direction of Ce 3d shifting is consistent with the electron doping. The Ce 3d XPS spectra show the presence of main peaks $4f^1$, satellite peaks $4f^2$ for Ce^{3+}, and satellite peaks $4f^0$ for Ce^{4+} valence.[38,39] It can be seen that $4f^0$ (Ce^{4+}) contribution from the $3d_{3/2}$ component
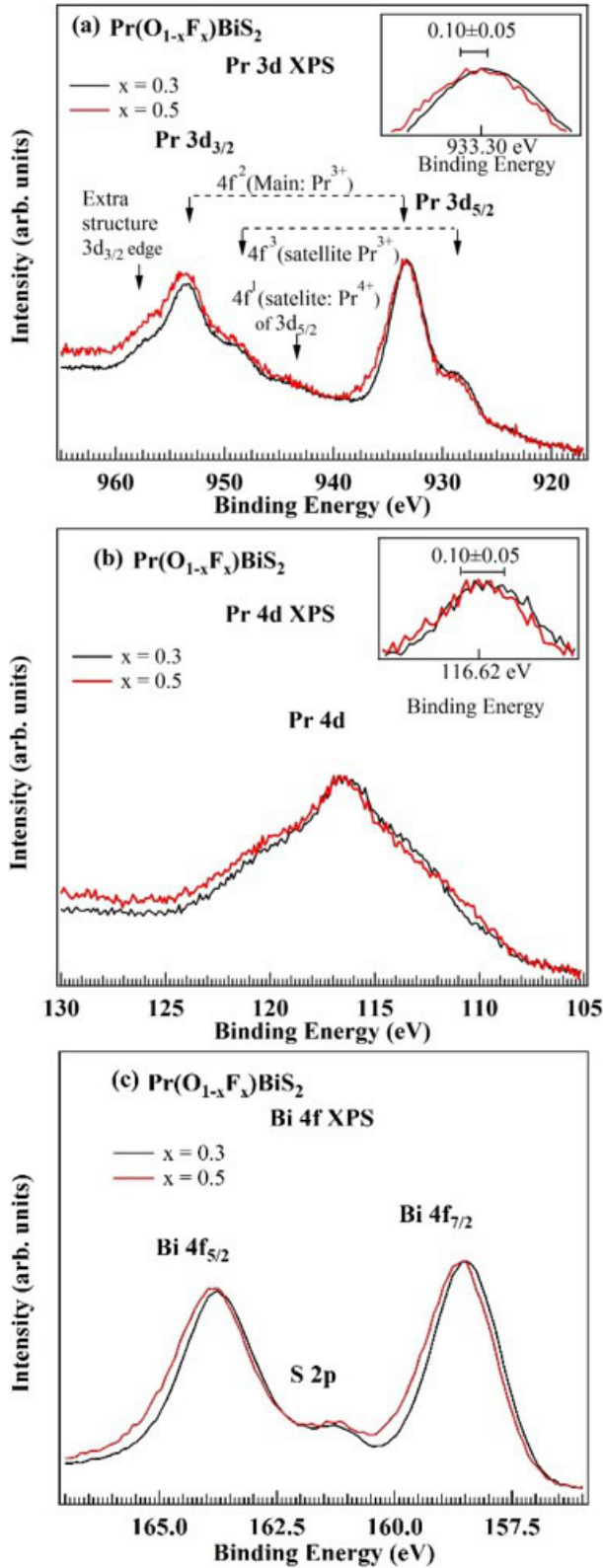
FIG. 3: (Color online) XPS of (a) Pr $3d$, (b) Pr $4d$, and (c) Bi $4f$ from $PrO_{1-x}F_xBiS_2$ ($x = 0.3$, 0.5) at room temperature.
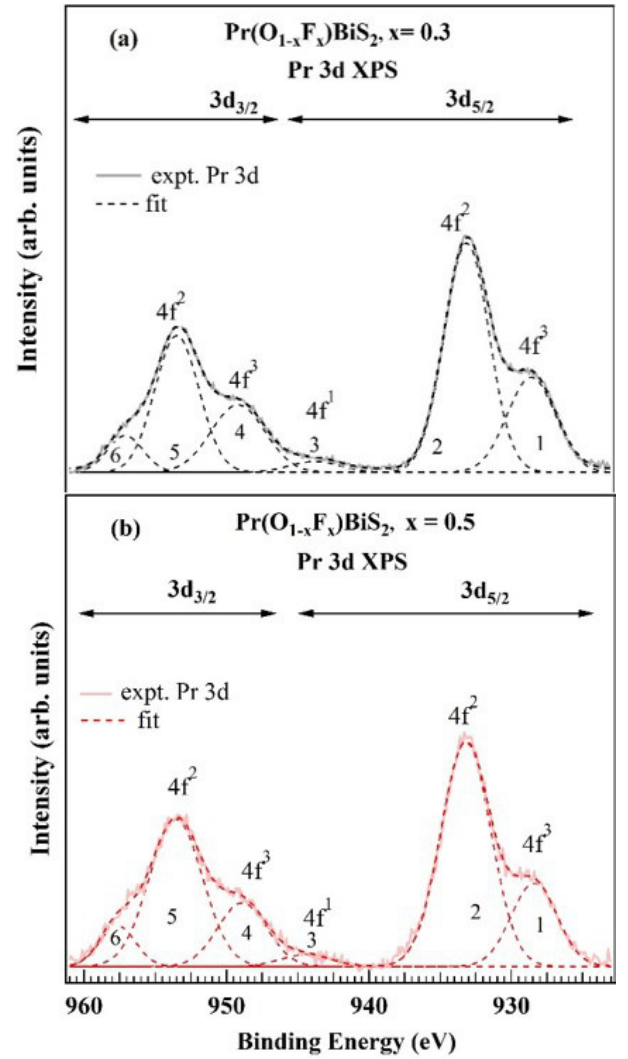
FIG. 4: (Color online) XPS of Pr $3d$ with Gaussian fittings from $PrO_{1-x}F_xBiS_2$ for (a) $x = 0.3$ and (b) $x = 0.5$ at room temperature.

is decreased with respect to $4f^1$ with doping, consistent with the earlier XAS study.[31] The detailed Ce $3d$ peak analysis of $CeO_{1-x}F_xBiS_2$ ($x = 0$, 0.5) is explained later in Fig. 2. As the resonant photoemission study earlier revealed that the F doping tunes the number of electrons mixed with localized Ce $4f$ in the Kondo regime instead of contributing to the Fermi surface,[36] a significant spectral weight transfer within the $4f^0$, $4f^1$, and $4f^2$ peaks of Ce $3d$ [Fig. 1(a)] with the electron doping can be seen. The initial states are given by $\alpha 4f^0 + \beta 4f^1 + \gamma 4f^2$ due to mixed valence ($\alpha^2 + \beta^2 + \gamma^2 = 1$). The final states are given by $\alpha' c4f^0 + \beta' c4f^1 + \gamma' c4f^2$, ($\alpha'^2 + \beta'^2 + \gamma'^2 = 1$) and c represents a core hole at the $3d$ level or at the $4d$ level.[38] The $4f^0$, $4f^1$, and $4f^2$ are different states with the U_{ff} (Coulomb repulsion between $4f$ electrons) and the U_{fc} (core hole interaction with $4f$ electrons). In Ce $4d$, apart from shifting towards high binding energy side [inset of Fig. 1(b)], the shoulder peaks around the main

peak $4f^1$ ($\sim$ 111 eV) in Fig. 1(b) vary with doping, indicating the importance of intra-atomic multiplet coupling and solid-state hybridization.[40] In Fig. 1(c), the Bi $4f$ peaks show a shift of $\sim$ 0.10 $\pm$ 0.01 eV towards high binding energy due to electron doping from $x = 0$ to 0.5 in $CeO_{1-x}F_xBiS_2$. The valence decrease of Ce with x should reduce the Ce $3d/4d$ binding energy. On the other hand, by adding electron at the valence band, all the core level peaks move away from the Fermi level with x as seen in Fig. 1. In the present case, the doping effect is dominant compared to the valence effect since the shift of Ce $3d$ is similar to that of Bi $4f$.

It was earlier reported that superconducting and ferromagnetic phase evolves with a different local environment in $CeO_{1-x}F_xBiS_2$ by suppressing Ce^{3+}/Ce^{4+} valence fluctuation.[37,41] In the self-doped Eu systems, Eu^{2+}/Eu^{3+} mixed valence is consistent with the photoemission results.[42] While in the Ce system, the doped electrons are partially localized and not consistent with the nominal x in $REO_{1-x}F_xBiS_2$. In this connection, the nature of valence states in $CeO_{1-x}F_xBiS_2$ ($x = 0$ to 0.5) are crucial and hence quantitatively evaluated in Fig. 2. Shirley type background is removed from the Ce $3d$ peaks of $CeO_{1-x}F_xBiS_2$ ($x = 0$, 0.5) and nine Gaussian peaks are fitted on the Ce $3d$. The Gaussian peaks are assigned for the $4f^2$, $4f^1$, and $4f^0$ contributions in Ce $3d_{5/2}$ and $3d_{3/2}$ from $CeO_{1-x}F_xBiS_2$ ($x = 0$, 0.5). The peaks are shifted by $\sim$ 0.10 $\pm$ 0.05 eV towards the higher binding energy from $x = 0$ to 0.5 in $CeO_{1-x}F_xBiS_2$. It shows that the intensity of $4f^0$ is almost suppressed while going from $x = 0$ [Fig. 2(a)] to $x = 0.5$ [Fig. 2(b)]. This is consistent with the previous XAS work by Sugimoto *et al.*[31] The Ce^{3+}/Ce^{4+} intensity ratio is evaluated from the relative intensity between $4f^1$ (Ce^{3+}) and $4f^0$ (Ce^{4+}) for Ce $3d_{5/2}$ indicated as peak 3 and 4 respectively in Fig. 2, and found almost two fold ($\sim$ 1.89) decrease in Ce^{4+} from $x = 0$ to 0.5.

In Fig. 3(a), the Pr $3d$ spectra of $PrO_{1-x}F_xBiS_2$ ($x = 0.3$ and 0.5) show shifting of $\sim$ 0.10 $\pm$ 0.05 eV towards higher binding energy by the F doping (inset). The direction of Pr $3d$ shifting is consistent with the electron doping. The spectral features of Pr $3d$ for $x = 0.3$ and 0.5 show similar features to the case of Pr_6O_{11}, where Pr^{3+} and Pr^{4+} coexist.[43] Pr $3d$ XPS from $PrO_{1-x}F_xBiS_2$ ($x = 0.3$, 0.5) show coexistence of Pr^{3+} and Pr^{4+} spectral features as shown in Fig. 3(a).[20,43–45] In Fig. 3(b), Pr $4d$ XPS have the shoulders around the main peak ($\sim$ 117 eV) showing a little change apart from shifting towards higher binding energy with the electron doping (inset). The interplay of intra-atomic multiplet coupling and solid-state hybridization can also be related with spectral features of $3d$ and $4d$ including the satellites.[40] However, the effect of the solid-state hybridization in Pr_6O_{11} and $PrO_{1-x}F_xBiS_2$ ($x = 0.3$ and 0.5) would be different. The solid-state hybridization is present between the $4f$ and O $2p$ with $4f^1\underline{L}$ and $4f^2\underline{L}^2$ charge transfer satellites where ($\underline{L}$) represents hole at the O $2p$.[38] In Fig. 3(c), the Bi $4f$ spectra show shift by $\sim$ 0.12 $\pm$ 0.01 eV towards higher
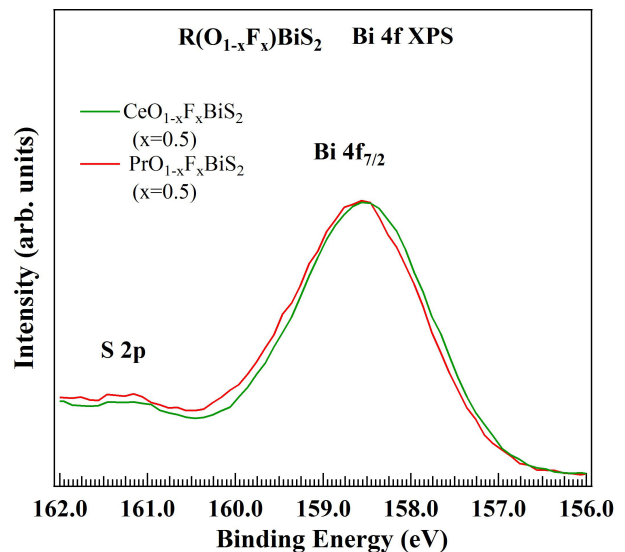
FIG. 5: (Color online) XPS of Bi $4f$ from $PrO_{1-x}F_xBiS_2$ and $CeO_{1-x}F_xBiS_2$ for $x = 0.5$ at room temperature.
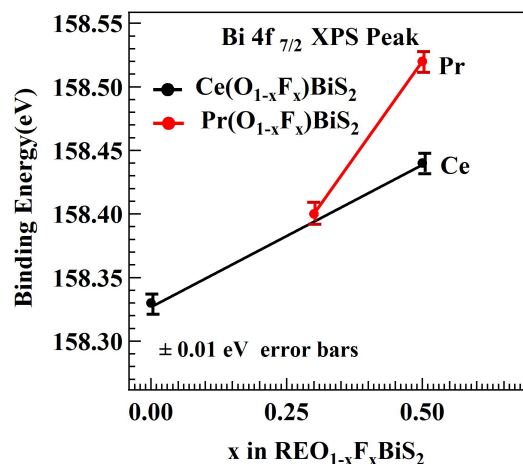
FIG. 6: (Color online) Position of Bi $4f_{7/2}$ obtained from Gaussian fitting from $PrO_{1-x}F_xBiS_2$ ($x=0.3$, 0.5) and $CeO_{1-x}F_xBiS_2$ ($x=0$, 0.5) at room temperature.

binding energy side from $x = 0.3$ to 0.5 for $PrO_{1-x}F_xBiS_2$ due to the electron doping.

The possibility of the Pr^{3+}/Pr^{4+} mixed valence was recently ascribed for $x = 0.13$ and 0.23 in $PrO_{1-x}F_xBiS_2$, and the spectral features were a bit ambiguous due to lack of detailed peak fitting study.[20] Therefore, we used multiple peaks to fit the Pr $3d$ of $PrO_{1-x}F_xBiS_2$ ($x = 0.3$, 0.5) in Fig. 4. The Pr $3d$ of $PrO_{1-x}F_xBiS_2$ ($x = 0.3$, 0.5) are subtracted by the Shirley type background and fitted with six Gaussians ascribing $4f^3$, $4f^2$, and $4f^1$ as shown in Figs. 4(a) and 4(b), respectively. The peak at $\sim$ 957 eV in the higher binding energy side of the Pr $3d_{3/2}$ from $PrO_{1-x}F_xBiS_2$ ($x = 0.3$, 0.5) is ascribed as an extra structure of $3d_{3/2}$.[40] Therefore, the Pr^{3+}/Pr^{4+}

intensity ratio is estimated from the peak area of $4f^2$ (Pr^{3+}) and $4f^1$ (Pr^{4+}) of Pr $3d_{5/2}$ shown as peak 2 and 3 respectively in Fig. 4. It was found that Pr^{3+}/Pr^{4+} is almost constant with the electron doping from $x = 0.3$ to 0.5. This shows that the addition of the electrons from $x = 0.3$ to 0.5 do not involve with the $4f^1$ (Pr^{4+}) and $4f^2$ (Pr^{3+}) components, rather only shifts the binding energy of the core levels away from the Fermi level.

In addition to this, Bi $4f_{7/2}$ peak shifts towards higher binding energy side from $CeO_{0.5}F_{0.5}BiS_2$ to $PrO_{0.5}F_{0.5}BiS_2$ at room temperature as shown in Fig. 5. The peak positions of Bi $4f_{7/2}$ obtained from Gaussians fitted on Bi $4f$ from $PrO_{1-x}F_xBiS_2$ (x=0.3, 0.5) and $CeO_{1-x}F_xBiS_2$ (x=0, 0.5) at room temperature are summarized in Fig. 6 and show shifting away from the Fermi level with the F doping. In $LaO_{1-x}F_xBiS_2$ (x=0 to 0.5),[46] the shift of the Bi $4f_{7/2}$ is around 0.3 eV with the electron doping similar to the case of shifting of the Bi $4f_{7/2}$ in Pr systems. While in the Ce systems, the Bi $4f_{7/2}$ shift is less compared to the Pr system (Fig. 6) and the Ce^{3+}/Ce^{4+} mixed valence is suppressed. The electron occupation to the $4f$ orbitals due to electron doping is different for the Ce and Pr systems. The shift in Ce $3d$ and Pr $3d$ with the electron doping were calculated from the Gaussians fitted as shown in Figs. 2 and 4. The Ce^{3+}/Ce^{4+} valence fluctuations is suppressed while Pr^{3+}/Pr^{4+} mixed valence remains unchanged by the F doping. In addition, the slope of the Bi $4f_{7/2}$ binding energy is larger in the Pr system than the Ce system. While the Ce valence is almost $+3$ at $x = 0.5$ in the Ce system, the Pr^{3+}/Pr^{4+} mixed valence still remains at $x = 0.5$ in the Pr system. The electron occupations to the $6p$ hybridized orbitals due to doping could be different for the Ce and Pr systems.

IV. CONCLUSION

We have studied the electronic structure of $CeO_{1-x}F_xBiS_2$ (x = 0, 0.5) and $PrO_{1-x}F_xBiS_2$ (x = 0.3, 0.5) by means of XPS. The core level photoemission spectra show shifts towards higher binding energy with the F doping. In $CeO_{1-x}F_xBiS_2$ (x = 0.5), the doped electrons suppress the Ce^{4+} contribution and valence fluctuation consistent to the early studies. The decrease in the valence fluctuation is associated with the decrease of Ce^{4+} components due to increase of Bi $6p_z$ orbital occupations by electron doping. The suppression of valence fluctuation is related to the onset of superconductivity in $CeO_{1-x}F_xBiS_2$ from $x = 0$ to 0.5. In $PrO_{1-x}F_xBiS_2$ (x=0.3, 0.5), the doped electrons do not suppress the Pr^{3+}/Pr^{4+} valence fluctuation. Rather, it increases the shifting of the Bi $4f_{7/2}$ away from the Fermi level higher and T_c is enhanced from x=0.3 to 0.5. However, Pr^{3+}/Pr^{4+} valence fluctuation still remains at $x = 0.5$ in the $PrO_{1-x}F_xBiS_2$. The difference in valence fluctuation between the Ce and Pr systems is associated with the difference in the magnetic properties.

V. ACKNOWLEDGMENT

[1] Y. Mizuguchi, H. Fujihisa, Y. Gotoh, K. Suzuki, H. Usui, K. Kuroki, S. Demura, Y. Takano, H. Izawa, and O. Miura, Phys. Rev. B **86**, 220510(R) (2012).

[2] S. K. Singh, A. Kumar, B. Gahtori, G. Sharma, S. Patnaik, and V. P. S. Awana, J. Am. Chem. Soc. **134**, 16504 (2012).

[3] Shruti, P. Srivastava, and S. Patnaik, J. Phys.: Condens. Matter 25, 312202 (2013).

[4] G. Baskaran, Supercond. Sci. Technol. 29, 124002 (2016).

[5] Y. Mizuguchi, S. Demura, K. Deguchi, Y. Takano, H. Fujihisa, Y. Gotoh, H. Izawa, O. Miura, J. Phys. Soc. Jpn. **81** 114725 (2012) .

[6] V. P. S. Awana, A. Kumar, R. Jha, S. K. Singh, A. Pal, Shruti, J. Saha, and S. Patnaik, Solid State Commun. **157**, 21 (2013).

[7] D. Yazici, K. Huang, B. D. White, A. H. Chang, A. J. Friedman, and M. B. Maple, Philos. Mag. **93**, 673 (2012).

[8] D. Yazici, et al., Phys. Rev. B **87**, 174512 (2013).

[9] R. Jha, A. Kumar, S.K. Singh, V.P.S. Awana, J. Supercond. Nov. Magn. **26** 499 (2013).

[10] R. Jha, A. Kumar, S. K. Singh, and V. P. S. Awana, J. Appl. Phys. **113**, 056102 (2013).

[11] K. Deguchi, Y. Mizuguchi, S. Demura, H. Hara, T. Watan- abe, S. J. Denholme, M. Fujioka, H. Okazaki, T. Ozaki, H. Takeya, . Yamaguchi, O. Miura, and Y. Takano, Europhys. Lett. **101**, 17004 (2013).

[12] S. Demura, Y. Mizuguchi, K. Deguchi, H. Okazaki, H. Hara, T. Watanabe, S. J. Denholme, M. Fujioka, T. Ozaki, H. Fujihisa, Y. Gotoh, O. Miura, T. Yamaguchi, H. Takeya, and Y. Takano, J. Phys. Soc. Jpn. **82**, 033708 (2013).

[13] J. Xing, S. Li, X. Ding, H. Yang, and H.-H. Wen, Phys. Rev. B **86** 214518 (2012).

[14] D. Yazici, I. Jeon, B. D. White, and M. B. Maple, Physica C **514**, 218236 (2015).

[15] S. Demura, K. Deguchi, Y. Mizuguchi, K. Sato, R. Honjyo, A. Yamashita, T. Yamaki, H. Hara, T. Watanabe, S. J. Denholme, M. Fujioka, H. Okazaki, T. Ozaki, O. Miura, T. Yamaguchi, H. Takeya, and Y. Takano, J. Phys. Soc. Jpn. **84**, 024709 (2015).

[16] R. Jha, H. Kishan, and V. P. S. Awana, J. Appl. Phys. **115**, 013902 (2014).

[17] R. Higashinaka, T. Asano, T. Nakashima, K. Fushiya, Y. Mizuguchi, O. Miura, T. D. Matsuda, and Y. Aoki, J. Phys. Soc. Jpn. **84**, 023702 (2015).

[18] M. Nagao, A. Miura, S. Watauchi, Y. Takano, and I.

Tanaka, Jpn. J. Appl. Phys. **54**, 083101 (2015).

[19] M. Nagao, Nov. Supercond. Mater. **1**, 6474 (2015).

[20] S. Ishii, Y. Hongu, A. Miura, and M. Nagao, Appl. Phys. Express **9**, 063101 (2016).

[21] Y. Mizuguchi, J. Physics. Chem. Solids **84**, 34-48 (2015).

[22] H. Usui, K. Suzuki, and K. Kuroki, Phys. Rev. B **86**, 220501(R) (2012).

[23] T. Sugimoto, D. Ootsuki, C. Morice, E. Artacho, S. S. Saxena, E. F. Schwier, M. Zheng, Y. Kojima, H. Iwasawa, K. Shimada, M. Arita, H. Namatame, M. Taniguchi, M. Takahashi, N. L. Saini, T. Asano, R. Higashinaka, T. D. Matsuda, Y. Aoki, and T. Mizokawa, Phys. Rev. B **92**, 041113(R) (2015).

[24] C. Morice, E. Artacho, S. E. Dutton, D. Molnar, H-J. Kim, and S. S. Saxena, J. Phys.: Condens. Matter **28**, 345504 (2016).

[25] G. Lamura, T. Shiroka, P. Bonfà, S. Sanna, R. De Renzi, C. Baines, H. Luetkens, J. Kajitani, Y. Mizuguchi, O. Miura, K. Deguchi, S. Demura, Y. Takano, and M. Putti, Phys, Rev. B **88**, 180509(R) (2013).

[26] B. Li, Z. W. Xing, and G. Q. Huang, Europhys. Lett. **101**, 47002 (2013).

[27] X. Wan, H. C. Ding, S. Y. Savrasov, C. G. Duan, Phys. Rev. B **87**, 115124 (2013).

[28] J. Lee, M. B. Stone, A. Huq, T. Yildirium, et al., Phys. Rev. B. **87**, 205134 (2013).

[29] T. Yildirim, Phys. Rev. B. **87**, 020506(R) (2013).

[30] Y. Wakisaka, K. Takubo, T. Sudayama, J.-Y.Son, T. Mizokawa, M. Arita, H. Namatame, M. Taniguchi, S. Sekiya, K. Fukuda, F. Ishikawa, and Y. Yamada, J. Phys. Soc. Jpn. **77**, 074710 (2008).

[31] T. Sugimoto, B. Joseph, E. Paris, A. Iadecola, T. Mizokawa, S. Demura, Y. Mizuguchi, Y. Takano, and N. L. Saini, Phys. Rev. B **89**, 201117(R) (2014).

[32] T. Agatsuma and T. Hotta, Journ. of Magn. and Magn. Mat. 400, 7380 (2016).

[33] T. Sugimoto, D. Ootsuki, C. Morice, E. Artacho, S. S. Saxena, E. F. Schwier, M. Zheng, Y. Kojima, H. Iwasawa, K. Shimada, M. Arita, H. Namatame, M. Taniguchi, M. Takahashi, N. L. Saini, T. Asano, R. Higashinaka, T. D. Matsuda, Y. Aoki, and T. Mizokawa Phys. Rev. B **92**, 041113(R) (2015).

[34] L. K. Zeng, X. B. Wang, J. Ma, P. Richard, S. M. Nie, H. M. Weng, N. L. Wang, Z. Wang, T. Qian, and H. Ding, Phys. Rev. B **90**, 054512 (2014).

[35] Z. R. Ye, H. F. Yang, D. W. Shen, J. Jiang, X. H. Niu, D. L. Feng, Y. P. Du, X. G. Wan, J. Z. Liu, X. Y. Zhu, H. H. Wen, and M. H. Jiang, Phys. Rev. B **90**, 045116 (2014).

[36] T. Sugimoto, D. Ootsuki, E. Paris, A. Iadecola, M. Salome, E. F. Schwier, H. Iwasawa, K. Shimada, T. Asano, R. Higashinaka, T. D. Matsuda, Y. Aoki, N. L. Saini, and T. Mizokawa, Phys. Rev. B **94**, 081106(R) (2016).

[37] E. Paris, B. Joseph, A. Iadecola, T. Sugimoto, L. Olivi, S. Demura, Y. Mizuguchi, Y. Takano, T. Mizokawa, and N. L. Saini, J. Phys.: Condens. Matter 26 435701 (2014).

[38] S. Hüfner, *Photoelectron Spectroscopy* (Springer-Verlag Berlin Heidelberg, 2003).

[39] A. Fujimori, Phys. Rev. B **28**, 2281(R) (1983).

[40] H. Ogasawara, A. Kotani, R. Potze, G. A. Sawatzky, and B. T. Thole, Phys. Rev. B **44**, 5465 (1991).

[41] M. Nagao, A. Miura, I. Ueta, S. Watauchi, I. Tanaka, Solid State Communications **245**, 1114 (2016).

[42] E. Paris, T. Sugimoto, T. Wakita, A. Barinov, K. Terashima, V. Kandyba, O. Proux, J. Kajitani, R. Higashinaka, T. D. Matsuda, Y. Aoki, T. Yokoya, T. Mizokawa, and N. L. Saini, Phys. Rev. B **95**, 035152 (2017).

[43] A. A. Yaremchenko, S. G. Patrício, J. R. Frade, journal. Power. Source **245**, 557-569 (2014).

[44] M. Y. Sinev, G. W. Graham, L. P. Haack, and M. Shelef, J. Mater. Res. **11**, 1960 (1996).

[45] S. Lütkehoff, M. Neumann, and A. Ślebarski, Phys. Rev. B **52**, 13808 (1995).

[46] S. Nagira, J. Sonoyama, T. Wakita, M. Sunagawa, Y. Izumi, T. Muro, H. Kumigashira, M. Oshima, K. Deguchi, H. Okazaki, Y. Takano, O. Miura, Y. Mizuguchi, K. Suzuki, H. Usui, K. Kuroki, K. Okada, Y. Muraoka, and T. Yokoya, J. Phys. Soc. Jpn. **83**, 033703 (2014).